

DTIC FILE COPY AD A109360 Trans 2067

UNLIMITED

Trans 2067

LEVEL II

BR81270

①



ROYAL AIRCRAFT ESTABLISHMENT

\*

Library Transtation 2067

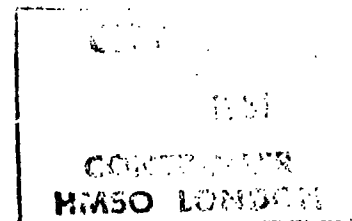
April 1981

DTIC  
ELECTE  
S JAN 07 1982 D  
E

# THE STRUCTURAL FORMATION AND PHYSICAL BEHAVIOUR OF CROSS-LINKED EPOXY RESINS

by

M. Fisher  
F. Lohse  
R. Schmid



\*

Procurement Executive, Ministry of Defence  
Farnborough, Hants

8112 31 023

UNLIMITED

Translations in this series are available  
from:

THE R.A.E. LIBRARY  
Q.4 BUILDING  
R.A.E. FARNBOROUGH  
HANTS

New translations are announced monthly in:

"LIST OF R.A.E. TECHNICAL REPORTS,  
TRANSLATIONS and BIBLIOGRAPHIES"

UDC 678.644 : 541.57 : 678.01 : 541.6 : 678.01 : 53

ROYAL AIRCRAFT ESTABLISHMENT

Library Translation 2067

Received for printing 6 April 1981

THE STRUCTURAL FORMATION AND PHYSICAL BEHAVIOUR OF  
CROSS-LINKED EPOXY RESINS

(STRUKTURELLER AUFBAU UND PHYSIKALISCHES VERHALTEN  
VERNETZTER EPOXIDHARZE),

by

M. Fisher

F. Lohse

R. Schmid

*Makromol. Chem.*, **181**, 1251-1287 (1980)

Published by Hüthig and Wepf Verlag, Basle, (Switzerland)

Translator

Barbara Crossland

Translation editor

W.W. Wright

AUTHORS' SUMMARY

Network structures and physical properties of products obtained either by crosslinking polyepoxides with polyphenols, and by dicyandiamide or by catalytic polymerization are discussed and compared with those obtained by amine or anhydride curing. The highest crosslinking density is achieved by the polymerization of epoxy compounds. In polymerization, the glass transition temperature may rise by more than  $\Delta T_{gv} = 100$  K. Amine and phenol curing result in similarly structured networks with mobile aliphatic segments and comparatively low crosslinking densities. Impact resistance based on dissipation of mechanical energy increases as network density decreases, a maximum being achieved with a medium chain length of 25-35 atom intervals between crosslinking points. The mechanical stability of polymers is limited by the cohesive strength  $KF$ . This latter corresponds to the maximum shear strength of bonds  $TKF_{max}$ , which was measured within the temperature range of 77 K to 450 K, in accordance with the equation

$$TKF_{max} = KF = B - C \cdot T; \quad T < T_g$$

This equation was derived from Eyring's model of viscosity, correlating  $B$  and  $C$  with activation volume, activation energy,  $T_g$  and strain rate.  $B$  equals the cohesive strength at 0 K. It is determined by intermolecular forces but does not depend on the density of crosslinking. An increase of  $T_g$  due to crosslinks or bulky segments causes a decrease of  $C$  and therefore a reduction of the temperature dependence of  $KF$ . Hence, cohesive strength at room temperature is improved.

LIST OF CONTENTS

	<u>Page</u>
1 INTRODUCTION	3
2 EFFECT OF THE CROSS-LINKED STRUCTURE ON POLYMER PROPERTIES	3
2.1 Effect of the type of cross-linking on the cross-linked structure	3
2.2 Effect of temperature on the cross-linking reaction	6
2.3 Effect of temperature on the cross-linked product	7
2.4 Relationship between cross-linked structure, cross-link density and glass transition temperature	7
2.5 Relationship between the cross-linked structure and mechanical properties	11
3 RELATIONSHIP BETWEEN STRUCTURE AND COHESIVE STRENGTH	12
3.1 Comparison of the torsional adhesive strength and the mechanical strength of mouldings	12
3.2 Cohesive strength of some epoxy resins of different structures	14
3.3 Significance of the temperature dependence of cohesive strength	15
3.4 Effect of the chemical structural unit on cohesive strength parameters	19
3.5 Plasticisation and cohesive strength	21
Tables 1 to 7	24
References	31
Illustrations	Figures 1-15

Accession For	
NTIS GRA&I	<input checked="" type="checkbox"/>
DTIC TAB	<input type="checkbox"/>
Unannounced	<input type="checkbox"/>
Justification	
By	
Distribution/	
Availability Codes	
Dist	Avail and/or Special
A	

## 1 INTRODUCTION

The epoxy resin polyaddition system, because of the many combination possibilities represents an ideal experimental field for the investigation of relationships between chemical structures and physical properties of cross-linked materials. Polyaddition reactions lead, when specific resins and curing agents are used, to a broad spectrum of materials ranging from glass/hard to rubber elastic and including different morphologies (crystallinity, different phases).

Many investigations into the effect of special structural features on the physical behaviour of polymers have been carried out on polyaddition systems using polyamines, dicarboxylic acid anhydrides and polycarboxylic acids<sup>1,2</sup>. Less well known are the cross-linked structures and properties which result upon curing with polyphenols and dicyandiamide and upon the polymerisation of epoxy compounds.

By way of examples using model compounds, the cross-linked structures of these three types of cure and their effect on physical behaviour are presented and compared with amine- and anhydride-type cures. The cross-linking reaction affects the chemical structure of the cross-links and the cross-link density. It therefore exerts a characteristic effect on the physical properties of the cross-linked polymer. Of basic importance for the understanding of mechanical behaviour is a knowledge of cohesive strength. The torsional adhesion test makes possible the determination of cohesive strength and its variation over a wide range of temperature for resins of different structure. This opens up interesting new possibilities for analysing the effect of structural parameters on cohesive strength and, in general on mechanical behaviour.

## 2 EFFECT OF THE CROSS-LINKED STRUCTURE ON POLYMER PROPERTIES

### 2.1 Effect of the type of cross-linking on the cross-linked structure

Since the basic reaction involved in the polyaddition of epoxy compounds has been extensively documented, a model of the cross-linked structure suitable for purposes of discussion can consist of schematic, segmental structural pictures, which can be used for the clarification of characteristic behaviour. Whereas a spatial representation<sup>3</sup> detracts from a clear grasp of the formula, the usual schematic two-dimensional illustration, lacking a third dimension, makes the average network values too small. Nevertheless, the basic facts concerning (a) the structure between cross-links, (b) the distance between cross-links and (c) the ratio of various structural elements to each other, are reproduced unchanged.

Before presenting the results of investigations, the different types of cross-link structure obtained using bisphenol A diglycidyl ether (BADG)\* together with mononuclear aromatic cross-linking (curing) agents will be illustrated. Of course, the principles involved in the structure formation can be applied also to other epoxy compounds and curing agents of the same type<sup>4,5</sup>.

---

\* Systematic IUPAC nomenclature: 2,2-bis-[4-(2,3 epoxypropoxy) phenyl]propane.

#### (a) Anhydride cross-linking

Cross-linking of BADG with dicarboxylic acid anhydrides having a cyclic anhydride structure<sup>6-9</sup>, leads to the formation of polyetherester structures (Fig 1), where the central C atom of the former glycidyl group\* comprises the cross-linking position within the longest (six-membered) aliphatic intermediate segment. This cross-linking position restricts the free movement of the segment, because the  $-O-$  or  $C=O$  groups at the ends of the segment are already bonded relatively rigidly to the aromatic nucleus.

In practice, one mole of anhydride and 0.1 to 1.0 wt.% of a tertiary amine (Benzyl dimethylamine etc) or of an imidazole (2-ethyl-4-methylimidazole, etc) as catalysts are introduced per epoxy equivalent and cross-linking is achieved by subsequent heat treatment (ca 3-20 h at 160°C, depending on the system).

Such polyetherester structures show, in general, a considerable resistance to oxidation, but a rather low resistance to humidity, particularly when hot. At temperatures of ca 330°C, these systems tend to degrade, i.e. anhydride components vaporise with the formation of partial polyether structures.

#### (b) Amine cross-linking

The addition of di- or poly-amines to bisphenol A diglycidylether gives rise to polymers with ether bridges and tertiary amino-groups<sup>10-12</sup>, where the nitrogen atoms represent the cross-linking positions (Fig 2). For each active N-H group, one glycidyl group is consumed; this is transformed into a five-membered intermediate segment with a central hydroxyl group which is inserted regularly between the aromatic structural units. In comparison with the system cross-linked with anhydride, the distances between cross-linking positions are greater here, and the  $-CH_2-\underset{\substack{| \\ OH}}{CH}-CH_2$  groups possess increased mobility<sup>1</sup>.

In contrast to anhydride systems, amine cross-linking requires mild curing conditions. At 160°C, a few minutes to a few hours are adequate for curing, depending on the formulation; aliphatic amines react even at room temperature. These polyetheramines are resistant to saponification, but are more liable to undergo oxidation reactions.

#### (c) Phenolic and acid cross-linking

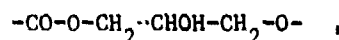
The treatment of phenolic hydroxyl groups<sup>13-15</sup> with diglycidylether leads to polyether structures in which, as shown in Fig 3, five-membered aliphatic intermediate chains alternate with aromatic structural units. The aromatic nucleus of the triphenol (phloroglucinol, pyrogallol) forms the cross-linking position. Due to the rigid bonding of the ether oxygen atom to the aromatic structure, high mobility is here again attributed to the  $-CH_2-CHOH-CH_2$  segment. Whereas in the case of cross-linking with primary aromatic diamines previously described, four chains proceed from the diamine, in the case of triphenol there are only three, hence the mesh size is increased quite considerably (doubled)<sup>2</sup>.

---

\* Glycidyl = 2,3 epoxypropyl

In order to ensure the desired course of the reaction 0.1 to 1.0 wt.% of accelerator must be added. Here again, imidazoles are to be preferred; however, tetramethylammonium chloride has the advantage that it does not initiate any concurrent polymerisation reaction. One phenolic hydroxyl equivalent is used for each epoxy group and complete cross-linking is achieved by heating to 160°C for ca 10-16 h.

A cross-linked structure comparable with that obtained with phenolic curing results when the cross-linking reaction involves polycarboxylic acids<sup>7,13,16</sup>. Instead of the phenyl ether oxygen atom, an ester group is introduced, and the intermediate aliphatic segment is extended by one chain link, the carbonyl group, giving the following structure:



and the flexibility of the polymer is increased. Since the majority of aromatic tri-carboxylic acids are high-melting substances, their application as curing agents imposes restrictions; they are therefore preferably used as oligoester derivatives in a powder system with triglycidylisocyanurate<sup>17\*</sup>. As cross-linked polyester derivatives, these structures, however, possess astonishingly good oxidation and saponification resistance.

#### (d) Catalytic cross-linking

When bisphenol A diglycidyl ethers are polymerised, preferably by Lewis acids<sup>18-20</sup> such as boron trifluoride etherate, boron trichloride-amine complex, tertiary amines or imidazole derivatives, polyethers result having structures comparable with those of a polypropylene glycol cross-linked through aromatic bridges (Fig 4). The cross-linked structure consists of more than half its molecular weight of aliphatic segments.

In contrast to the case of olefinic polymerisation, here between 1 and 10 wt.% of initiator is required. From this, and also from mechanical measurements on the polymerisate and analytical investigations on monoglycidyl compounds<sup>21</sup> it is found that the 'polypropylene'-chains are relatively short. The degree of polymerisation amounts, depending on the initiator used, to ca 5-15. Since, however, diglycidyl compounds are always used in practice, this 'disadvantage' is largely cancelled out. The cross-linking by polymerisation depends rather more on the type of initiator than on its concentration (see also TGA - values in Table 1). Larger additions (>6 wt.%) moreover, have the effect of increasing the flexibility of the cross-linked system.

#### (e) Dicyandiamide cross-linking

Structure formation reactions with dicyandiamide follow a complex pattern. Not only is one concerned with the addition reaction between the active hydrogen atoms<sup>22,23</sup> of this compound and the glycidyl groups available, but, according to more recent investigations<sup>24</sup>, one must consider cleavage of the dicyandiamide with the production of 2-aminooxazoline derivatives, in accordance with Fig 5. The structural scheme here is greatly simplified; there are indications that, in the course of the addition reaction, glycidyl groups can

\* Systematic IUPAC name: 1,3,5,-tris(2,3-epoxypropyl)-1,3,5-perhydrotriazine-2,4,6-trione.

attach themselves to free hydroxyl groups of the oxazoline derivative, with formation of ether bridges.

Epoxy resins can be converted practically completely using dicyandiamide without accelerator. The addition reaction can, however, be accelerated by the introduction of tertiary amines or imidazoles.

## 2.2 Effect of temperature on the cross-linking reaction

The structure of the components, and particularly the type of curing agent, determines the rate and temperature of the curing reaction. The temperature  $T_{RG(max)}$  from the DSC analysis, at which the heat evolution reaches a maximum, may be used for purposes of characterisation.

Aliphatic polyamines react more quickly than the other curing agents listed in Table 1. At a heating rate of  $8^{\circ}\text{C}$  per minute, the maximum exotherm is at a  $T_{RG(max)}$  of  $90^{\circ}\text{C}$ ; the corresponding temperatures for curing with aromatic amines lie between  $150\text{--}160^{\circ}\text{C}$ . Whereas catalysed cross-linking reaction with hexahydrophthalic acid anhydride and the cross-linking by polymerisation show  $T_{RG(max)}$  values between  $120\text{--}130^{\circ}\text{C}$ , the catalysed cross-linking reactions with polyphenols and the uncatalysed cross-linking reaction with dicyandiamide are extremely slow, and show  $T_{RG(max)}$  values of ca  $185^{\circ}\text{C}$  and  $200\text{--}210^{\circ}\text{C}$  respectively. The curing temperatures used lie, on average,  $20^{\circ}\text{C}$  below these values.

As a measure of the temperature dependence of the reaction rate, the activation energy  $E_a$  was obtained in  $\text{J} \cdot \text{mol}^{-1}$  from DSC measurements using different heating rates, and the following equation derived by Flynn and Wall<sup>25</sup>:

$$E_a \approx \left( 18.3 \frac{\text{J}}{\text{mol} \cdot \text{K}} \right) \cdot \frac{-d \log \beta}{d \frac{1}{T_{RG(max)}}} \quad (1)$$

where  $\beta$  = rate of heating in arbitrary units,

$T_{RG(max)}$  is in K.

According to experiment, the type of cross-linking reaction (see Table 1) affects the activation energy more than does the chemical structure of the resin and hardener. The cross-linking reaction with amines and phenols proceeds with relatively small activation energies of  $50\text{--}60 \text{ kJ/mole}$ , both in the case of reactive aliphatic and of slow-reacting aromatic amines. Therefore aliphatic amines afford the possibility of carrying out the curing of bisphenol A diglycidyl ethers at room temperature, provided that total curing of the system is not prevented by vitrification (raising of the glass transition temperature as the result of increased cross-linking density)<sup>26</sup>.

The  $E_a$  values of polymerisation cross-linking initiated by 1-methylimidazole lie rather higher at  $60\text{--}70 \text{ kJ/mole}$ . The effect of the quantity of catalyst is small, as comparative measurements using 2 and 4 wt.% show.



Higher  $E_a$  values are recorded for the cross-linking of epoxy compounds low in hydroxyl content with pure anhydrides. Such systems, catalysed with 1-methylimidazole, give values of 85 kJ/mole; furthermore, they have the advantage that the maximum cure rate is achieved only after an induction period, i.e. after completion of a slow preliminary reaction<sup>27</sup>. The highest activation energy is shown by the dicyandiamide curing agent. Its value of 137 kJ/mole, however, can, at least in part, be attributed to the insolubility of the hardener in bisphenol A diglycidylether, since the reaction only attains a faster rate when the finely suspended dicyandiamide has dissolved in the resin. This provides a means of producing resin/hardener systems stable to ageing.

### 2.3 Effect of temperature on the cross-linked product

The thermal stability of the cross-linked material is determined by its structure. In Table 1, test values are summarised for thermogravimetric analyses (TGA)<sup>28</sup> of the structural types previously described. For a heating rate of 4°C/min, there is observed, in the majority of cases, a small preliminary peak and, after a further temperature rise of 60-80°C, the main peak. Here the preliminary peak may arise through thermal breakdown of side chains, which finally no longer carry the functional groups involved in the reaction.

Cross-linked structures containing aliphatic polyamines as structural units show the lowest degradation temperature of 320°C. This temperature is about 80°C lower than is observed for phenolic cross-linking or polymerisation initiated with 1-methylimidazole. Anhydride systems are increasingly prone to scission, particularly if phthalic acid or hydrated phthalic acid derivatives are used as hardeners. Roughly the same stability is shown by products arising from cross-linking with aromatic amines (decomposition temperature  $\approx$  390°C) and with dicyandiamide (decomposition temperature  $\approx$  375°C).

### 2.4 Relationship between cross-linked structure, cross-link density and glass transition temperature

A characteristic and technically important parameter for amorphous polymers is the glass transition temperature  $T_g$ . This is not only critical for dimensional stability under heat, but it also has a crucial effect on most of the physical properties of the polymer at room temperature. There are various structural factors which influence the position of the  $T_g$ <sup>29-31</sup>. Thus a high polarity delays the introduction of free mobility of the chains upon heating. Equally as important, however, is the influence of so-called bulky segments, such as cyclic structural units, or space-filling substituents. These can cause  $T_g$  increases of up to 100°C. The same effect is also exerted by cross-linking which similarly hinders segment mobility because of bonding in three, or indeed four, directions. In the case of highly cross-linked epoxy resins,  $T_g$  increases of 20-100°C, or in particular cases even of about 200°C, are caused by the cross-linking process. This increase in  $T_g$  in comparison with linear polymers having the same structural units, which can be achieved by cross-linking is of vital importance for many applications. The  $T_g$  increase, or the cross-linking contribution  $\Delta T_{gv}$  in °C, can conveniently be evaluated using the simple empirical relationship<sup>27,29</sup>:

$$\Delta T_{gv} = \frac{788}{n_c} \quad (2)$$

Here,  $n_c$  is the mean number of atoms or the mean number of the atomic distances in the segments between two cross-linking positions, this latter number being taken as a basis for the  $\Delta T_{gv}$ -calculation subsequently to be carried out.

$T_g$ -determinations can be carried out by various methods, *eg* calorimetric analysis (DTA, DSC), thermomechanical analysis (TMA), torsional vibration analysis (TVA), determination of the dimensional stability under heat (*eg* ISO R 75 or VSM 77 137) or by way of the change in volume with rise in temperature. The  $T_g$  values obtained depend on the method used and on the pretreatment of the polymer. The differences between values found for the various methods are not the same for all polymers.

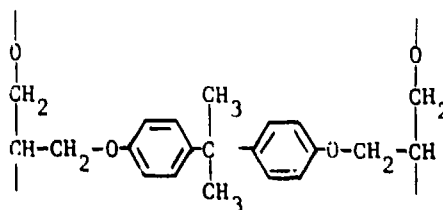
In Table 2, the  $T_g$  values given are those obtained by thermomechanical analysis, taking the temperature of maximum velocity of penetration of a loaded probe (rate of heating =  $10^\circ\text{C}/\text{min}$ , thickness of specimen = 1 mm).

The cross-link density, or the mean distance between two cross-linking positions  $n_c$  is, as stated in preceding sections, dependent on the type of hardener, even if hardeners of comparable structure are used. Although cross-linking of bisphenol A diglycidyl ether does not lead to a particularly highly cross-linked product, the cross-linking contributions for triphenol ( $33^\circ\text{C}$ ) and polymerisation cross-linking ( $108^\circ\text{C}$ ) calculated according to equation (2) show a considerable difference (Table 2).

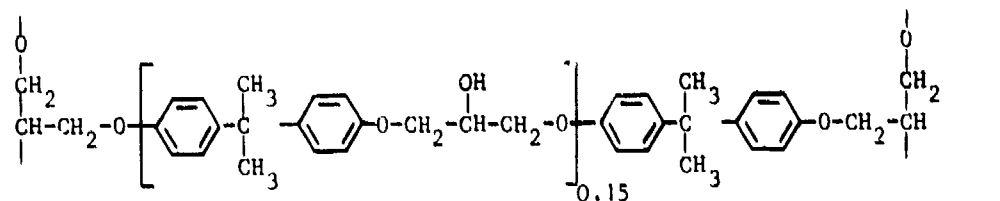
The  $T_g$  of a linear polymer of bisphenol A diglycidylether and resorcinol which is not cross-linked is about  $75^\circ\text{C}$ . Structurally similar linear systems, for example those produced using an aromatic diamine or an aromatic dicarboxylic acid, should have practically the same value. Their synthesis is, in fact, beset with numerous problems. Table 2 shows that the cross-linking contribution calculated according to equation (2) agrees very well with the measured difference,  $T_g(\text{cross-linked}) - T_g(\text{linear})$ , in the case of the anhydride system. For phenolic and particularly for amine systems, the glass transition temperatures measured lie above the values to be expected on the basis of the structure or of the cross-link density. It is assumed that the reason for this phenomenon lies in the free mobility of the intermediate aliphatic segments at room temperature, and that there is therefore a relationship with the well-defined  $\beta$ -relaxation of amine and phenolic systems<sup>32,33,1</sup>.

Bisphenol A diglycidyl ether cross-linked by polymerisation contains a rather larger content of aliphatic structural units, each of which shows two cross-linking positions.

The calculation of  $\Delta T_{gv}$  from equation (2) can advantageously be undertaken on the structural unit illustrated in Fig 4,



Since commercial bisphenol A diglycidyl ethers contain small amounts of higher molecular weight products\*, the following unit is to be regarded as the repeating one:



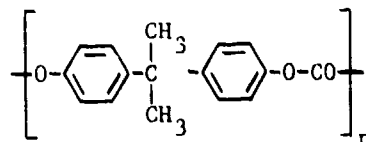
It is constructed from three segments between four cross-linking positions and from this,  $n_c$  is calculated as follows:

$$n_c = [3 + (2 + \{14 \times 0.15\} + 12) + 3] / 3 \approx 22/3 \approx 7.3$$

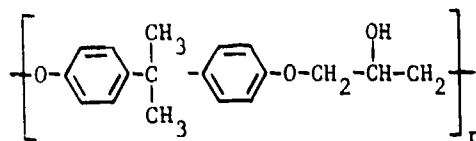
According to equation (2) a  $\Delta T_g$  value of  $108^\circ\text{C}$  therefore results. Using the  $T_g$  of the cross-linked polymer [ $T_g$  (cross-linked)], the associated hypothetical linear macromolecule is found to have a  $T_g$  of:

$$\begin{aligned} T_g(\text{linear}) &= T_g(\text{cross-linked}) - \Delta T_{gv} \\ &= 170 - 108 = 62^\circ\text{C} \end{aligned} \quad (3)$$

The calculated value of  $62^\circ\text{C}$  is quite realistic. The repeating unit contains the same structural element as a polycarbonate:



having a  $T_g$  of  $140^\circ\text{C}$  and a phenoxy:



with a  $T_g$  of  $90^\circ\text{C}$ ; however, the aliphatic content of the intermediate unit in the hypothetical structure is higher than in the latter case.

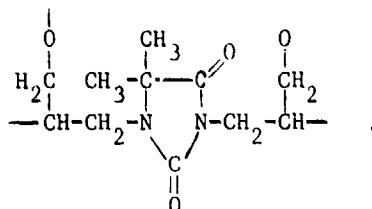
The high  $T_g$  value expected for catalytic hardening is, as Fig 6 illustrates, achieved only with some specific catalysts, such as 1-methylimidazole (MIL) or 2-ethyl-4-methylimidazole (EMI). When bisphenol A diglycidylether is polymerised using boron

\* These are addition products of the reaction between bisphenol A and BADG formed in small quantities during the synthesis of the glycidyl derivative of bisphenol A.

fluoride-amine complexes, it gives a  $T_g$  value which is some  $40^\circ\text{C}$  lower, whereas, if tertiary amines, eg tris(2,4,6-dimethylaminomethyl)-phenol are used to obtain the polymer, the value is lower still by about a further  $40^\circ\text{C}$ .

In the latter case, the low modulus of shear measured in the rubber-elastic state indicates incomplete cross-linking. In Fig 7 the effect of increasing quantities of initiator (MIL in wt.%) on the modulus of shear and on the glass transition temperature of the cross-linked material is shown. High concentrations of catalyst or initiator obviously bring about a reduction in the glass transition temperature, very probably due to chain-scission reactions.

It is very interesting to compare the curves for the modulus of shear associated with bisphenol A diglycidylether polymerised with 1-methylimidazole (MIL) and with 1,3-diglycidyl-5,5-dimethylhydantoin\*. If, using the glycidyl derivative of hydantoin, a polymerisation cross-linked structure, similar to that in Fig 4, is synthesised, the following basic unit is recognised:

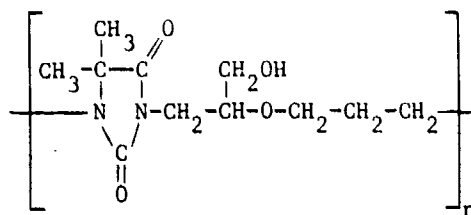


For this, according to equation (2):

$$T_{gv} = \frac{788}{(3 + 6 + 3)/3} = 197^\circ\text{C}.$$

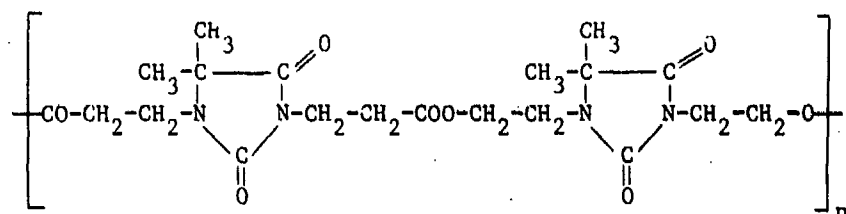
This relatively high value is due to the small distance between the two glycidyl groups in the molecule.

The strongly polar structure of the hydantoin residue appears to be responsible for the generally higher level of the modulus of shear. For a hypothetical linear polymer:



according to equation (3), a calculated value of  $T_g(\text{linear}) = 18^\circ\text{C}$  is found, a value which is perhaps reasonable when one considers that the glass transition temperature of oligoesters of the following structure:

\* Systematic IUPAC name: 1,3-bis(2,3-epoxypropyl)-5,5-dimethylimidazolidine-2,4-dione.



lies at 25°C.

Even if the application of equation (2) to such high cross-link densities is questionable, since, for various reasons (chain scission, problems associated with the collision of suitably reactive groups in the growing macromolecule, impurities) the theoretical cross-linked structure is unlikely to be produced, it nevertheless makes possible the determination of approximate  $T_g$  values which are adequate for many evaluation purposes. A calculation of the glass transition temperature from empirical incremental values is questionable, also, since appropriate values are not obtainable for every structure, the individual increments vary for different polymers and the effect of substituents on the glass transition is still not fully understood.

## 2.5 Relationship between the cross-linked structure and mechanical properties

A meaningful description of the mechanical behaviour of a cross-linked polymer as a function of temperature is given by curves such as those presented in Fig 8 for a system based upon bisphenol A diglycidylether, cross-linked with hexahydrophthalic anhydride, and catalysed by base. In the higher temperature region ( $>160^\circ\text{C}$ ), where there is a low modulus of shear  $G$ , the material possesses rubber-elastic properties with limited extensibility and small tensile strength. In the glass transition region,  $G$  increases sharply; the polymer now exhibits visco-elastic behaviour, and the mechanical damping and (as shown in Fig 8) the extensibility pass through a clearly-defined maximum, while the tensile strength increases, at first, rapidly, but then at a decreasing rate<sup>34,35</sup>. High tensile strength values are therefore attainable only at moderate temperatures sufficiently removed from the  $T_g$  interval, and necessarily at the expense of low extensibility.

In Table 3, a summary is given of the mechanical properties and the glass transition temperatures of the most important structural systems represented schematically in Figs 1 to 5. Certain facts should now be explained. Apart from the materials cross-linked catalytically (systems Nos. 11-16), all examples show good flexural strength at room temperature. Highly cross-linked epoxy resins, such as those obtained by catalytic polymerisation or by anhydride cross-linking, particularly when epoxy novolaks (EPN) are used, tend increasingly to undergo brittle fracture (systems Nos. 4, 14 and 15). The effect of the mobile intermediate segments on flexibility and impact strength is considerably reduced by the high cross-link density (cf systems Nos. 8 and 9, or 20 and 21).

The epoxy resins cross-linked with aromatic amines or phenols, possess high impact strengths. Here it seems that the flexible intermediate members spaced uniformly, make it possible for the impact energy to be quickly dissipated. High values of this kind

cannot themselves be attained by the direct introduction of plasticisers into hard, highly cross-linked systems, even when a considerable reduction in the glass transition temperature is associated with the process. In general, as shown in Fig 9, an increase in impact toughness occurs for comparable structures, with a rise in  $n_c$ , (that is by a reduction in the cross-link density), up to  $n_c \approx 25-35$ . The values for amine and phenolic cures lie on the same curve. Even with a favourable cross-linked structure, no success has been achieved in attaining a high impact strength and high cross-link density simultaneously. With a further increase in the value of  $n_c$  there is no increase in the impact toughness; a slight fall may even be observed.

The effect of the polarity of the cross-linking structural unit can be shown, eg by the cross-linking of heterocyclic epoxy compounds with 1,3-diglycidyl-5,5-dimethylhydantoin. Here it must be borne in mind that, due to the smaller distance between the two glycidyl groups, smaller mesh sizes result, and this again affects the physical behaviour.

### 3 RELATIONSHIP BETWEEN STRUCTURE AND COHESIVE STRENGTH

#### 3.1 Comparison of the torsional adhesive strength and the mechanical strength of mouldings

A valuable insight into the mechanical behaviour of polymers is afforded by the temperature dependence of the torsional adhesive strength, TAS. The torsional adhesion test is particularly suitable for the testing of curable polymers.

For this purpose, five hollow cylinders (external diameter  $2R_a = 12$  mm, generally of aluminium) are stuck using the resin of interest to a strong plate. The test equipment makes it possible to introduce a continuously increasing torsional moment ( $\dot{M} = 0.5 \text{ Nms}^{-1}$ ) into the adhesive bond with the help of the six-sided tube seen in Fig 10. The shear stress in the adhesive layer increases until rupture occurs. Assuming approximately elastic behaviour, the maximum shear stress can be calculated from the maximum torsional moment applied<sup>36</sup>,

$$\text{TAS} = \frac{2}{\pi} \frac{R_a \dot{M}}{R_a^4 - R_i^4} = \frac{2\dot{M}}{\pi R_a^3} \quad \text{when } R_i \ll R_a \quad (4)$$

where  $R_a$  = external radius of the cylinder  
 $R_i$  = internal radius of the cylinder.

By way of a lever arm to which the cemented plate is rigidly fixed, the rotational moment acts on a transducer. An x-t recorder registers the signal from the transducer. In parallel with this, the signal is passed to a computer for evaluation, by way of a voltmeter connected in the circuit. A thermostatic device makes it possible to achieve temperatures between  $-80^\circ\text{C}$  and  $+160^\circ\text{C}$ .

For measurements at  $-196^\circ\text{C}$ , the test-piece is immersed in liquid nitrogen. The simple cementing of specimens and the large temperature range investigated during testing are considerable advantages of the torsional adhesive technique<sup>36</sup>. Within experimental error, results agree with the torsional strength of cemented aluminium tubes ( $R_a = 70$  mm,  $R_i = 60$  mm)<sup>37</sup>.

Fig 11 shows the curves for the torsional adhesive strength (TAS) of aluminium cylinders on aluminium plates, in comparison with the tensile (TS) and flexural strength (FS) of mouldings as a function of temperature. To prepare the test-piece, equivalent quantities of BADG and hexahydrophthalic anhydride are mixed with 1 wt.% of accelerator and cured for 2 h at 180°C.

Below the  $T_g$  (see the arrow in Fig 11), the TAS, TS and FS increase with falling temperature. However, it is a striking feature that the test values for cast test-pieces lie, at -20°C, below the extrapolated curves. The stress-strain curves in Fig 12 explain this behaviour. Below the  $T_g$ , the strength initially increases with falling temperature as the result of the increasing resistance of the polymer to deformation. The stress-strain curve recorded at -20°C has no point with a horizontal tangent (yield point) such as those shown by the other three curves. At -20°C, rupture of the material occurs before the yield stress is reached (brittle fracture). In the case of TAS, on the other hand, the rise in value continues steadily at lower temperatures and, at -196°C, a value of 208 N mm<sup>-2</sup> is attained (see Table 4 and Fig 15). According to experience, the strength of polymers increases with increasing difference of the test temperature from the glass transition temperature  $T_g^{27,38-41}$ ; however, it proves extremely difficult to reach the yield point at low temperatures in a tensile or bending test. The situation is different in the case of the torsional adhesive test; provided that the TAS of a material increases uniformly with increasing difference of the test temperature from the  $T_g$ , it may be concluded that, below the shear stress, the polymer is 'fluid' and hence the yield point has been reached. The bonding has then failed cohesively. In this case, the TAS measures a material property characteristic of the polymer, namely the cohesive strength. If adhesive failures (failures at the interface) or small flaws in the adhesive had been responsible for the failure of the bonding, then the strength would not increase - or not to the same extent as before - with falling temperature. Under such circumstances, the TAS-temperature diagram is, from a certain strength value (the adhesive strength), approximately independent of temperature or it may even decrease at lower temperatures<sup>36</sup>. In Fig 11, the TS agrees roughly with the TAS in value, when a break does not occur before the yield stress (cohesive strength) is reached. The FS values, as expected, exceed the TS and TAS. The evaluation of the bending test takes as its basis the model of simple beam bending (J. Bernoulli). For large deformations, the assumptions<sup>42</sup> required to validate this model are not fulfilled, however, so that the calculation overestimates the stresses in the edge zones of the bending bar. The curve of TAS as a function of the temperature  $T$ , as presented in Fig 11, can be expressed with sufficient accuracy by a straight line (see Fig 15). The equation of such a line is:

$$TAS = C(T_g + A - T) \quad , \quad (5)$$

where  $C$  is the slope and  $T_g + A$  denotes the intercept on the abscissa. For the straight line through the test points in Fig 11,  $C = 0.59 \text{ N mm}^{-2} \text{ K}^{-1}$  and  $A = 38 \text{ K}$  (see Table 4 below).

The TAS for cohesive failure of the joint is denoted by  $TAS_{max}$ . It is the highest value of the TAS attained at the associated temperature. It is reached only if the joint does not break prematurely as the result of adhesive or brittle fracture.

### 3.2 Cohesive strength of some epoxy resins of different structures

The relationship between  $TAS_{max}$  and the test temperature  $T$  is confirmed by quite different epoxy resin systems. Thus the results in Fig 13 relate to four different types of cure: aromatic amine, aliphatic amine (TMD = isomeric mixture of 2,2,4- and 2,4,4-trimethylhexamethylenediamine, 50:50 wt.%), catalytic polymerisation and anhydride.

Fig 14 shows the TAS-temperature curve for different diglycidyl ethers (polypropyleneglycol-, bisphenol-A-, 5,5-dimethylhydantoin-); all specimens were hardened with aromatic amine. As in the case of Fig 11, a line is drawn through the plotted TAS test points and the characteristic values of  $C$  and  $(A + T_g)$  are calculated according to equation (5) for each polymer. Together with values for other systems, they form the contents of tables 4, 6 and 7.

Fig 15 summarises the behaviour over the whole temperature range 0 K to 500 K. It shows the effect of two plasticisers on the TAS of the system BADG + hexahydrophthalic anhydride.

Even though the points for TAS measurements at 77 K do not lie exactly on the line drawn for the cohesive strength, the good proportionality which continues down to low temperatures is surprising. In Table 4, the TAS values measured at 77 K are compared with the extrapolated cohesive strength values for the same temperature. The extrapolation is based on TAS measurements between the  $T_g$  and  $-80^\circ\text{C}$ . The agreement is very good. In two cases, the TAS measured lies above the extrapolated value; for the remaining systems, experimental values are only at most 6% below the expected strengths. As regards the increasing tendency for brittle or adhesive fractures to occur at such low temperatures, the deviations are within the experimental limits. It therefore appears reasonable to extrapolate also over the remaining 77 K down to absolute zero. For the  $TAS_{max}$  at 0 K, therefore, according to equation (5), one obtains:

$$TAS_{max}(0) = C(\hat{T}_g + A) \equiv B \quad (6)$$

Here  $\hat{T}_g$  is the glass transition temperature measured on the absolute scale of temperature:  $\hat{T}_g = T_g + 273 \text{ K}$ .  $B$  corresponds to the intersection on the ordinate of the straight lines in Fig 15. It represents an interesting value as a measurement of the cohesive strength at 0 K. Values of  $B$  for epoxy resins of different structures are given in Tables 4, 6 and 7. The accuracy of the  $B$ -values is essentially determined by the TAS results used for extrapolation. The margin of error for the extrapolation is seldom more than  $\pm 2\%$ . So far, it has not been possible to verify values for  $B$  experimentally; however, cohesive strengths of  $182\text{--}293 \text{ N mm}^{-2}$  at 0 K appear to be reasonable compared with test results for the flexural strength at 4.2 K. For a system formed from BADG and cycloaliphatic anhydride, a  $FS = 263 \text{ N mm}^{-2}$  is given, and, for BADG hardened with aliphatic amines, the FS lies between  $258$  and  $293 \text{ N mm}^{-2}$ <sup>43</sup>. With the help of the cohesive strength parameter  $B$  at 0 K introduced in equation (6), equation (5) can be written in the simple form:

$$TAS_{max} = CS = B - C.T \quad (7)$$



where  $T$  denotes the absolute temperature and  $CS$  the cohesive strength of the polymer.

Secondary relaxations are not taken into consideration where the temperature dependence of the cohesive strength is concerned. It is known, however, that the aliphatic linking segments formed when amine, phenolic or acid curing is employed, give rise to clearly defined  $\beta$ -relaxations. Consequently, the curve of the modulus of shear in the range of the  $\beta$ -relaxation ( $-45^{\circ}\text{C}$ ) shows a greater decrease when the relaxation amounts to about 3-4 dB. Therefore the  $TAS$  value for systems with a clearly defined  $\beta$ -relaxation in the region between  $-30^{\circ}\text{C}$  and the  $T_g$  is rather lower than the value corresponding to equation (5). An example of these deviations is afforded by the 1,3-diglycidyl-5,5-dimethylhydantoin and the 4,4'-diaminodiphenylmethane systems in Fig 14. Since the  $TAS$  measurements are available down to  $-80^{\circ}\text{C}$  or even to  $-196^{\circ}\text{C}$ , well below the temperature of the  $\beta$ -relaxation, it can be considered that the lines shown largely eliminate the effect of  $\beta$ -relaxation.

### 3.3 Significance of the temperature dependence of cohesive strength

Experiments having shown that  $TAS_{\text{max}}$  results in many cases can be described, with good approximation over a wide range of temperature, by the simple relationship in equation (7) the question arises as to the physical significance of this finding.

The preceding discussion has proposed the yield stress as a measurement of the cohesive strength. In the stress-strain curve, the yield strength is a clearly defined maximum and is very reproducible from the point of view of measurement, provided, of course, that the test-piece has not already fractured at a smaller stress. The yield process denotes a flow of the material at a given rate of deformation under constant stress. Tests at different temperatures and rates of deformation to determine the yield-behaviour of glass-like plastics<sup>40,44-46</sup> have shown that an activated process is involved here, as in the case of a melt. Deformations occur in a stepwise manner as the result of the rearrangement of many segments of the statistically disordered macromolecules. When new molecular configurations are formed, thermal energy assists the rearrangements of chain segments, while intramolecular rotation potential barriers and the neighbouring molecules mainly hinder such rearrangements. These concepts receive detailed treatment in the models of Robertson<sup>47</sup> and Argon<sup>48-50</sup>.

Occasionally, however,<sup>38,44-46,51,52</sup> the (generalised) Eyring concepts<sup>53</sup> for the viscosity of a liquid are simply applied to the yield processes. Although it must remain undecided whether this model makes possible an adequate description of experimental results in all cases<sup>54</sup>, without doubt its simplicity is enticing. Moreover, it receives convincing confirmation through the explanation of the temperature dependence of the cohesive strength.

The frequency  $\nu$  with which a molecular segment jumps over a potential barrier of height  $u$  into a neighbouring potential valley is<sup>53</sup>:

$$\nu = \nu_0 \exp \frac{-u}{kT} \quad (8)$$

where  $u$  = activation energy per unit;  
 $T$  = absolute temperature;  
 $k = 1.38 \times 10^{-23} \text{ J K}^{-1}$  (Boltzmann constant);  
 $\nu_0$  = characteristic frequency.

If a mechanical stress acts on the material, the rearrangement of segments is favoured in its direction. On the other hand, rearrangements in the opposite direction are made energetically more difficult. The difference between the activation energies introduced in equation (8) is:

$$\Delta u = \pm \tau n v$$

where  $\tau$  denotes the operative shear stress and  $nv$  denotes the volume participating in the rearrangement ( $v$  being the characteristic volume and  $n$  the number of participating units).

In the yield process, the material flows under the shear stress  $\tau_Y$  with a shear velocity  $\dot{\gamma}$ . For this, the model concept:

$$\dot{\gamma} = P \left( \exp \frac{-u}{kT} \right) \sinh \frac{nv\tau_Y}{kT} \quad (10)$$

has been considered<sup>55</sup>.

In addition to the known values, there is a further material-dependent constant of proportionality  $P$ . In the event that  $x$  of the function  $\sinh x$  is large in comparison with 1 ( $x \gg 1$ ), then approximately:

$$\sinh x = \left( \frac{1}{2} \right) (e^x - e^{-x}) \approx \left( \frac{1}{2} \right) e^x. \quad (11)$$

Therefore, under the condition that:

$$nv\tau_Y \gg kT \quad (12)$$

equation (10) can also be written:

$$\dot{\gamma} = \frac{P}{2} \exp \frac{-u + nv\tau_Y}{kT} \quad (13)$$

Equation (13) can be solved in terms of the yield stress:

$$\tau_Y = \frac{u}{nv} - T \frac{k}{nv} \ln \frac{P}{2\dot{\gamma}} \quad (14)$$

If, for the cohesive strength  $CS$  in equation (7), the yield stress  $\tau_Y$  is similarly introduced,

$$\tau_Y = B - TC \quad (7a)$$

then the similarity of the forms of equations (7a) and (14) can immediately be recognised.

A comparison of the corresponding coefficients gives the two equations:

$$B = \frac{u}{nv} \quad (15)$$

$$C = \frac{k}{nv} \ln \frac{P}{2\dot{\gamma}} \quad (16)$$

Accordingly, from the Eyring model a dependence of the yield stress  $\tau_y$  on the temperature  $T$  is found as shown by the torsional adhesive strength test. The model interprets the value  $B$  (see equation (6)) as the activation energy  $u$  of a molecular segment, divided by the volume  $nv$  (activation volume, see equation (15)) participating in the rearrangement. The value  $C$  (slope of the TAS-temperature curve) relates the model (see equation (16)) to  $nv$  and to the logarithm of the ratio of two shearing velocities;  $\dot{\gamma}$  denotes the shearing velocity at which the test is carried out;  $P$  denotes a less distinct material-dependent constant.

Since the model advanced for the cohesive strength has proved successful, the numerical values of the parameters  $u$ ,  $nv$  and  $P$  contained in the model are of interest. Measurements of TAS could be carried out only at the test velocity ( $\dot{\gamma} \approx 0.01 \text{ s}^{-1}$ ) and therefore afforded only the two values  $\tau_y$  and  $T$  for three unknowns. Therefore reference was made to an example in the literature in order to determine the numerical values of  $u$ ,  $nv$  and  $P$  for polycarbonates, using the test results obtained by Bauwens-Crowet, Bauwens and Homes<sup>44</sup>. In accordance with Figs 13 and 14, the yield stresses  $\tau_y$  for three different rates of elongation in the tensile test  $\dot{\epsilon}$  were plotted against temperature. Straight lines can be drawn through the points, and from these lines were calculated the values for  $A$ ,  $B$  and  $C$  given in Table 5 ( $T_g = 145^\circ\text{C}$ ).

According to Table 5, the value  $B$  is practically independent of the rate of elongation  $\dot{\epsilon}$  ( $B = 158 \text{ N mm}^{-2}$ ). The experiment thus confirms the information provided by the model (equation (15)) that the cohesive strength at 0 K depends only on the activation energy  $u$  and the activation volume  $nv$ .

Using the values for  $B$ ,  $C$  and  $\dot{\epsilon}$  from Table 5, the required values of  $u$ ,  $nv$  and  $P$  can be calculated from equations (15) and (16)\*. The activation energy per unit,  $u = 4.8 \times 10^{-19} \text{ J}$ ; the activation volume,  $nv = 3.0 \times 10^{-27} \text{ m}^3$ ; the constant  $P = 1.2 \times 10^{28} \text{ s}^{-1}$ .

The value of the activation energy of 290 kJ/mole (69 kcal/mole) found is somewhat lower than the value of 75.5 kcal/mole quoted in the literature<sup>44</sup>. The activation energies of the viscosity of comparable melts vary within these values.

The activation volume is about ten times the volume of a monomer unit. It agrees with the explanation<sup>53,56</sup> that, when rearrangement of a molecular segment occurs,

---

\* From equation (16), one obtains:

$$P = 2\dot{\epsilon}_k^{1-x_k} \dot{\epsilon}_l^{x_l} \quad (17)$$

where  $x = C_k/C_l - C_l$

$k$  and  $l$  denote the numbers 1, 2 and 3 in Table 5.

several monomer units are involved. This finds expression also in the relatively large activation energy.

According to experiment, the (Newtonian) viscosities of glasses at their respective glass transition temperature agree within certain limits<sup>57,58</sup>. By virtue of this fact, a second possible method arises for the determination of the constant  $P$ .

The (Newtonian) viscosity  $\eta$  is found, from equation (10) as a function of the temperature  $T$ , insofar as

$$nv\tau_Y \ll kT \quad (18)$$

when the shear stress  $\tau_Y$  is vanishingly small. The series expansion  $\sinh x + x^3/3! + \dots$  can then be discontinued after the first term:

$$\eta = \lim_{\tau \rightarrow 0} \frac{\tau}{\dot{\gamma}} = \frac{kT}{nv} \cdot \frac{1}{P} \exp \frac{u}{kT} \quad (19)$$

The required value of  $P$  follows from equation (19), if the viscosity  $\eta(T_g)$  at the glass transition temperature  $\hat{T}_g$ , measured on the absolute temperature scale, is introduced.

$$P = \frac{k\hat{T}_g}{nv\eta(T_g)} \exp \frac{u}{k\hat{T}_g} \quad (20)$$

where  $u$  = activation energy  
 $nv$  = activation volume.

With the help of equation (20),  $P$  can be eliminated from equation (16) (where  $\hat{T}_g$  is in K):

$$C = \frac{u}{nv} \frac{1}{\hat{T}_g} + \frac{k}{nv} \ln \frac{k\hat{T}_g}{2\dot{\gamma}\eta(T_g)nv} \quad (21)$$

A logical connection has therefore been shown between the experimental values  $A$ ,  $B$ ,  $C$  and the glass transition temperature  $\hat{T}_g$  and also between the molecular parameters (activation energy  $u$ , activation volume  $nv$ ). For the glass transition temperature ( $\hat{T}_g$  in K), one obtains:

$$\hat{T}_g = \frac{B}{C + \frac{k}{nv} \ln \frac{2\dot{\gamma}\eta(T_g)nv}{k\hat{T}_g}} \quad (22)$$

From equations (15), (21) and (22), the following important conclusions can be drawn:

(a) the glass transition temperature  $T_g$  is, according to equation (22), high in the case of polymers having flat TAS versus  $T$  curves and a high strength at 0 K.

(b) A high strength of 0 K is, according to equation (15) to be expected for polymers with a large activation energy and a small activation volume.

(c) By reducing the deformation rate  $\dot{\gamma}$ , the slope of the TAS versus T diagram increases (according to equation (21), C becomes greater).

(d) For polymers having a high activation energy and polymers having a small activation volume, the curves are comparatively steep (according to equation (21), C becomes large).

### 3.4 Effect of the chemical structural unit on cohesive strength parameters

As examples of the most important structures in epoxy-resin cross-linked materials (see section 2.1), typical hardener and resin units are summarised in Table 6.

For each example, the following values are given:

- (1)  $T_g$ , the glass transition temperature (by TMA) (see section 2.4).
- (2) C, the slope of the schematic TAS versus temperature curve. According to equation (7), C can be regarded as the negative temperature coefficient of the cohesive strength, CS :

$$C = - \frac{d(CS)}{dT} . \quad (23)$$

Values of C lie between  $0.36 \text{ N mm}^{-2} \text{ K}^{-1}$  and  $0.88 \text{ N mm}^{-2} \text{ K}^{-1}$ , although, in the majority of examples, they lie between 0.5 and  $0.6 \text{ N mm}^{-2} \text{ K}^{-1}$ .

- (3) B, the cohesive strength CS of the polymer at 0 K. Values of B lie between 182 and  $293 \text{ N mm}^{-2}$ .

- (4) A, the interval between the experimentally determined  $T_g$  (TMA) and the temperature B/C, for which the TAS in the schematic description is equal to 0 ( $\hat{T}_g$  in K):

$$A = \frac{B}{C} - \hat{T}_g . \quad (24)$$

Since C (see equation (21)), and also the  $T_g$  depend on test conditions (rate, prehistory) and are, therefore, subject to a degree of uncertainty, A is adequately defined only in relation to the test situation. In the examples chosen, the value for A varies between 11 K and 87 K, although a typical value is 40 K.

The following discussion is intended, with the aid of a comparison of the 17 different systems considered in Table 6, to show the extent to which the chemical structure affects the cohesive strength. As a reasonable, if not actually a representative, reference system, the set of mean values for the 17 systems is taken.

According to equation (7), the parameters B and C are all important where the cohesive strength is concerned. Systems having values of B and C, which differ from the mean values of  $\bar{B} = 253 \text{ N mm}^{-2}$  and  $\bar{C} = 0.56 \text{ N mm}^{-2} \text{ K}^{-1}$  by not more than  $\pm 6\%$ , include Nos. 1, 10, 13, 14 and 16 as representatives of the five different types of cure,

and also the phenoxy resin (system No.15) which is not cross-linked. From this it may be concluded that  $B$ , and hence the cohesive strength at 0 K, are hardly affected by the type and density of cross-linking. On the other hand, cross-linking and the associated increase in the glass transition temperature  $T_g$  (see section 2.4) for an otherwise similar structure, gives rise to rather lower  $C$  values as a comparison of systems Nos. 15 and 14, for a glance at equation (21) shows. Thus a higher degree of cross-linking and a higher  $T_g$  at a median temperature, i.e. in the region of room temperature up to the  $T_g$ , results in greater cohesive strength.

Curing with dicyandiamide leads to strikingly high values of  $A$ . A similar value of  $A$  is also achieved in the case of the formulated product AV 13b (without filler) HV 998 in Table 4. The technical importance of high  $A$  values lies in the possibility of achieving good strengths even under comparatively mild curing conditions a little below the  $T_g$ . Other examples in Table 6 show the way in which the chemical structure of the unit affects the cohesive strength.

In system No.11, one is dealing with a non-polar, extremely bulky and immobile molecular skeleton. The activation volume, at  $\nu \approx 30 \text{ nm}^3$ , is about ten times greater than that of polycarbonate or an epoxy resin based on bisphenol A. The cohesive strength  $B$  at 0 K is comparatively small; since, however, due to the large activation volume (see equation (21)),  $C$  is also small, the system has a usable strength over a wide range of temperature. The effect of high 'bulkiness' is therefore comparable with that of a high cross-link density. In both cases, mobility is restricted.

For the same structure and cross-link density, a polymer having a considerably higher  $T_g$  results if, in the hardener of systems Nos.1, 2, the  $-\text{CH}_2-$  group is replaced by the bulkier  $-\text{SO}_2-$  group (see systems Nos.6,7). Here again, a decrease in the  $C$ -value and hence an improvement in cohesive strength in the middle of the temperature range is associated with an increase in the  $T_g$ .

The polarity of the structural unit is found to be of decisive importance where the cohesive strength of the polymer at low temperatures is concerned.  $B$  rises clearly, for example, if BADGE in systems Nos.1, 4 and 6 in Table 6 is replaced by hydantoin diglycidylether (systems Nos.2, 5, 7). If *m*-phenylene-diamine is used instead of the hardener 4,4'-diaminodiphenylmethane, causing an increase in the concentration of nitrogen and hydroxyl groups in the polymer, and hence the polarity, then the value of  $B$  also increases. On the other hand, curing with trimethylhexamethylenediamine (an isomeric mixture of 2,2,4- and 2,4,4-trimethylhexamethylenediamine (50:50 wt.%) brings about a reduction in  $B$  and  $C$ , due to the weak polarity involved. The same resin hardened with triethylenetetramine\*, however, (system No.8) results in the formation of a polymer with increased hydroxyl group concentration and hence with higher polarity. For this reason, system No.8 gives higher  $B$  and  $C$  values than system No.9.

In general, high polarity of the structural unit produces a larger  $C$  value. In the case of epoxy resins with a lower  $T_g$ , this finds particularly good expression in

---

\* Systematic IUPAC name: 3,6-diazooctan-1,8-diamine.

equation (21). Thus, polypropyleneglycoldiglycidylether (molecular weight 572) in system No.3 is characterised by a high B-value and a strikingly large C value.

The examples given taking structural units of different polarities show the way in which the Van der Waals forces between molecular segments determine the cohesive strength B at 0 K. The experimental findings are in accord with the evidence of equation (15) which relates the cohesive strength B and the energy density, that is the ratio of the activation energy u to the activation volume nv.

For epoxy resins, a typical value of  $B = u/(nv) = 250 \text{ N/mm}^2 = 250 \text{ MJ/m}^3$  is obtained.

During combination of molecules in the liquid or solid phase, the cohesive energy  $E_{\text{coh}}$  is marked by a change in the internal free energy. The cohesive energy of liquids can be determined experimentally from the heat of vaporisation<sup>59</sup>. In the case of polymers on the other hand, the cohesive energy can be determined only indirectly from swelling tests, or on the basis of the first law of thermodynamics, and data concerning this value<sup>60</sup> have sometimes shown considerable variation. For the cohesive energy density:

$$\delta^2 = \frac{E_{\text{coh}}}{V_{\text{mol}}} \quad (25)$$

( $E_{\text{coh}}$  = molar energy of cohesion;  $V_{\text{mol}}$  = molar volume); and from the comprehensive table of van Krevelen and Hoftyzer<sup>60</sup>, for polymethylmethacrylate at room temperature,  $345 \text{ MJ m}^{-3} < \delta^2 < 687 \text{ MJ m}^{-3}$ , and for an epoxy resin not defined in detail<sup>61</sup>,  $\delta^2 = 500 \text{ MJ m}^{-3}$ . Extrapolation to the cohesive energy at 0 K involves, according to Bondi<sup>61</sup>, relatively small corrections.

The cohesive strength B varies within the same order of magnitude as the cohesive energy density  $\delta^2$  which, according to its definition, is again an expression of inter-molecular forces.

When the yield process occurs in a loaded polymer, that is when the activation volume nv has at its disposal an activation energy u, and when the molecules can be displaced in relation to each other, the molecules are still in a liquid-like combination possessing a certain cohesive energy. The cohesive energy density  $\delta^2$  at 0 K should therefore be greater than the cohesive strength B by an amount corresponding to this fluidity. In fact the B-values measured (see Table 6) ( $182 \text{ MJ m}^{-3}$  up to  $293 \text{ MJ m}^{-3}$ ) lie below the cohesive energy densities ( $\delta^2 \approx 500 \text{ MJ m}^{-3}$ ) to be expected for these polymers.

### 3.5 Plasticisation and cohesive strength

In the preceding sections, the effect of structure on the thermal and mechanical behaviour of polymers was discussed. Possibilities of variations in the case of epoxy resins, however, are not exhausted. The addition of fillers or plasticisers makes it possible to modify technical products further, so that the morphology (in the wider sense) is changed. Homogeneous materials in themselves have not always satisfied the various requirements.

As an example of the effect of morphology, the way in which four different plasticisers introduced into the system BADG + hexahydrophthalic anhydride act on the glass transition temperature  $T_g$ , the flexural strength FS, the crack toughness  $K_{IC}$ , the torsional adhesive strength TAS and on the parameters B and C of the cohesive strength is summarised in Table 7. The critical stress intensity factor  $K_{IC}$  (fracture toughness) was determined from the load which, in the three-point bending test, causes further growth in the crack previously introduced into the test-piece<sup>63</sup>. The knowledge of fracture toughness is important to the fabricator in his choice of material. Materials having large  $K_{IC}$ -values enable a higher loading to be applied to the designed item than to one made from less tough materials if the size of a possible defect is assumed to be the same in both cases<sup>64</sup>.

By the introduction of 15 wt.% of adipic acid polyester into the cross-linked structure, the cross-link density falls as also does the  $T_g$  (by 15 K). Plasticisation by means of polyesters based on dimerised aliphatic acids leads to partial phase separation, because of the differing polarities of resin and plasticiser. Phase separation occurs still more markedly when the non-polar butadiene-acrylonitrile copolymer is used as the plasticiser. The diameter of the rubber-elastic inclusions is about 1  $\mu\text{m}$ <sup>65,66</sup>. These three plasticisers are introduced into the cross-linked system through carboxyl end groups. Their effect on the cross-link density is such that they extend the glass transition range to lower temperatures.

In contrast, ABS powder contains no reactive groups. The small particles are embedded like a filler in the cross-linked resin and remain as a separate phase. The  $T_g$  of the epoxy resin is not affected by the introduction of the second phase (ABS).

The effect of plasticisation on mechanical properties is worth noting; as the result of the addition of only 15 wt.% of a non-polar plasticiser, the cohesive strength at 0 K falls from  $B = 262$  to  $B = 194 \text{ N mm}^{-2}$ . The value of C falls also, from 0.59 to  $0.45 \text{ N mm}^{-2} \text{ K}^{-1}$ . This observation is in agreement with equation (21).

Fig 15 shows the curve for the strength (TAS) over a wide temperature range of specimens plasticised in different ways.

- $T_g$  does not vary essentially, so that all TAS versus T lines intersect the T-axis at about the same point.
- As the polarity decreases, the cohesive strength of the polymer falls.
- The strength of plasticised polymers is reduced by the same ratio for all temperatures between 0 K and the  $T_g$ .

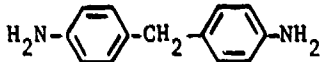
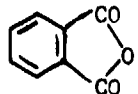
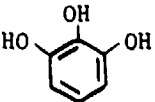
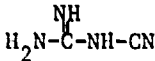
In agreement with discussions in section 3.4, the examples in Table 7 also show the sensitivity of the two parameters B and C of the cohesive strength to a weakening of the intermolecular (Van der Waals) forces. Associated with this is a decrease in the flexural strength and the torsional adhesive strength of approximately 25%. Opposed to this is a gain in the fracture toughness as the result of plasticisation. The  $K_{IC}$ -values in Table 7 are more than doubled if the plasticiser is present as a separate, finely-divided phase. As a result of this, a crack grows in a plasticised resin only



when the load is twice as great as that needed for crack growth in a non-plasticised resin under the same conditions. In contrast to the mechanical properties, the fracture toughness  $K_{IC}$  shows no dependence on cohesive strength. It appears, rather, that fracture toughness is determined by the morphology, whereas the molecular structure is responsible for cohesive strength. The cohesive strength and fracture toughness therefore have a dual relationship. The model discussed for cohesive strength explains the relationship between chemical structure and the physical behaviour of an epoxy resin over a wide range of temperature. It provides, however, no information concerning fracture toughness.

Table 1

Effect of the type of hardener on the thermal properties of cross-linked, bisphenol A diglycidylether ( $T_{RG(max)}$  = temperature of the maximum reaction rate for a heating rate of  $8^{\circ}\text{C/min}$ ;  $E_a$  = activation energy of the polyaddition derived from  $T_{RG(max)}$  according to equation (1)).

Curing agent	DSC analysis (a)		TGA (b)		Main peak °C
	T <sub>RG(max)</sub> °C	E <sub>a</sub> kJ/mole	Preliminary peak (c)		
	°C		°C	%	
	157	50	-	0	390
Trimethylhexamethylenediamine	90	59	-	0	320
 (d)	125	91	333	12	392
Polymerisation with 1-methylimidazole:					
2 wt.%	126	67	342	3.2	420
4 wt.%	123	67	344	4.7	416
 (e)	185	55	343	2.9	400
	207	137	-	0	373

(a) DSC = differential scanning calorimetry.

(b) TGA = thermogravimetric analysis. Thickness of moulding = 1 mm.  
Heating rate:  $4^{\circ}\text{C/min}$ .

(c) Peak from the time derivative of the weight/temperature (time) curve (maximum rate of vaporisation). The percentage weight loss is obtained from the weight/temperature curve.

Acceleration with

(d) 0.2 wt.% benzyldimethylamine.

(e) 0.1 wt.% methylimidazole.

Table 2

Effect of the type of curing on the cross-link density and glass transition temperature  $T_g$  of cross-linked, bisphenol A diglycidylether (BADG); ( $n_c$  = mean number of atomic distances between two cross-linking positions;  $\Delta T_g$  (calculated) =  $T_g$ -displacement, governed by the cross-linking, calculated according to equation (2);  $\Delta T_g$  (measured) =  $T_g$ -displacement, governed by the cross-linking, determined according to  $T_g$  (measured) =  $T_g$  (TMA) -  $T_g$  (linear);  $T_g$  (linear) =  $T_g$  of polymers of analogous structure, not cross-linked; for amine, phenolic, and anhydride curing of BADG  $\approx 75^\circ\text{C}$ ).

Hardener					
$n_c$	10.7	14.7	24	7.3	14
$T_g$ (TMA) / $^\circ\text{C}$ (b)	146	148	120	170	120
$\Delta T_g$ (calc) / $^\circ\text{C}$	73	54	33	108	56
$\Delta T_g$ (measured) / $^\circ\text{C}$	71	73	45	-	(45) (c)

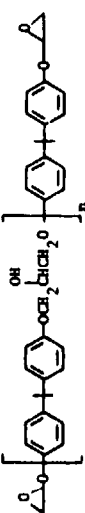
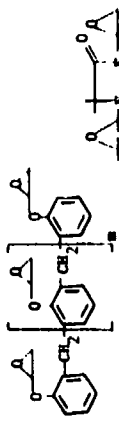
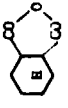
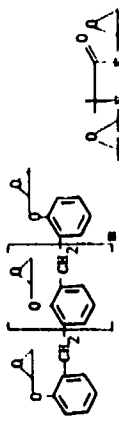
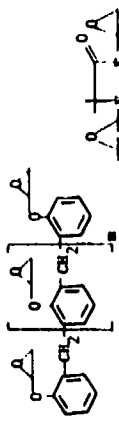
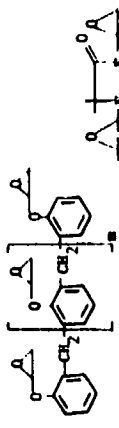
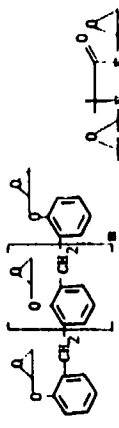
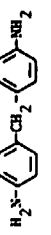
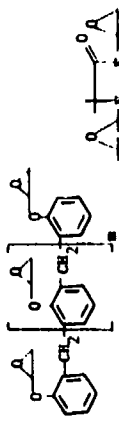
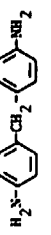
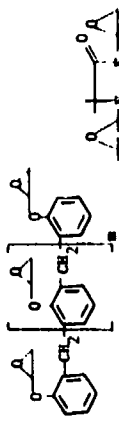
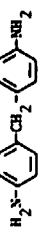
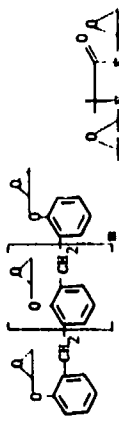
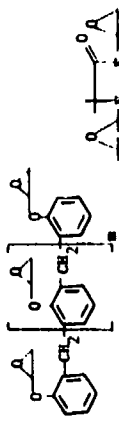
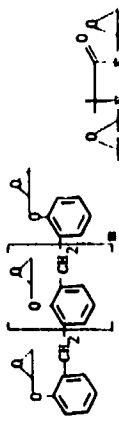
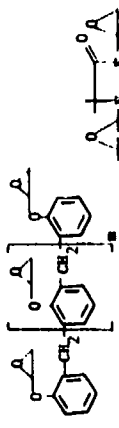
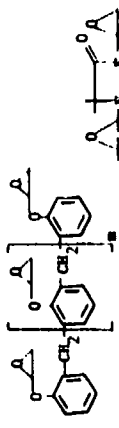
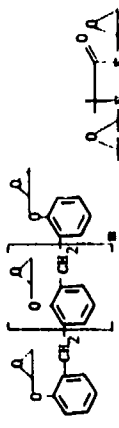
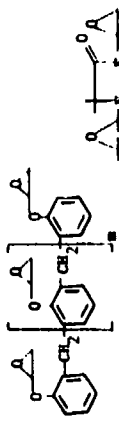
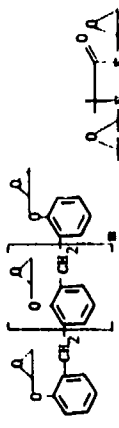
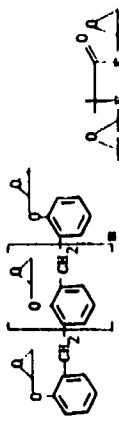
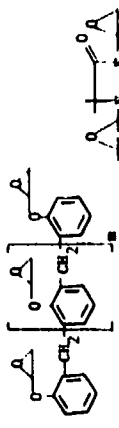
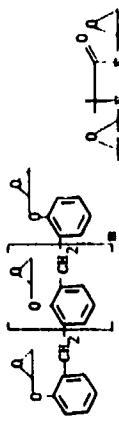
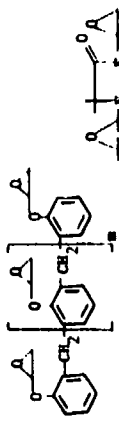
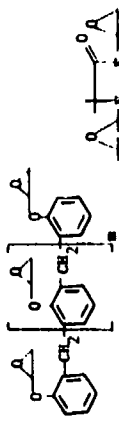
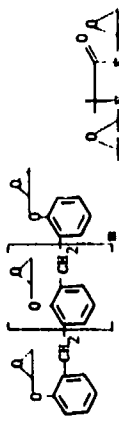
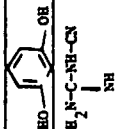
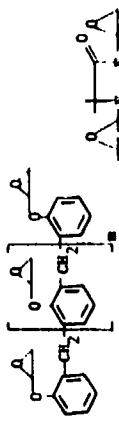
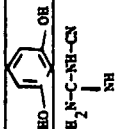
(a) acceleration with tetramethylammonium chloride.

(b) TMA = thermomechanical analysis.

(c) extrapolated value.

Table 3

Effect of the cross-linked structure on the glass transition temperature  $T_g$  of epoxy resins (determined as the thermal dimensional stability according to VSN 77161) and the mechanical behaviour of cured epoxy resins ( $n_c$  = mean number of atomic distances in the main chain between two cross-linking positions;  $\Delta T_g = T_g$ -displacement, calculated according to equation (2))

No.	Epoxy resin (basic structure)	Curing with	$n_c$	$\Delta T_g$ °C	$T_g$ °C	FS N mm <sup>-2</sup>	DB mm	SB N mm <sup>-1</sup>
1 2			10.7	73	130	136	12	25
3			19	42	115	132	14	46
4			8.8	89	137	152	10	26
5			6.8	116	158	152	8	17
6			7.3	107	173	160	8	17
7			17	47	159	135	14	54
8			34	23	123	138	15	78
9			11.3	70	170	150	12	37
10			8.5	93	194	132	7	24
11			10	79	186	191	12	25
12			7.3	108	170	115	6	16
13			7.3	108	142	114	6	13
14			16	48	112	111	10	20
15			5.0	157	166	107	4	11
16			4.1	192	196	103	4	6
17			4.0	197	188	106	3	4
18			24	33	120	126	16	73
19			50	16	103	123	17	73
20			14	56	116	148	6	11
21			17	47	120	153	12	64
22			11	72	148	143	9	25
23			22	36	106	150	13	69
			14	56	120	158	6	21

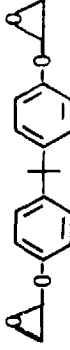
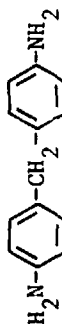
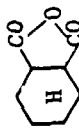
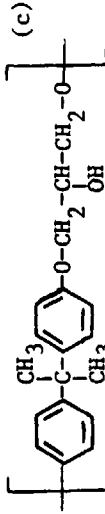
FS = flexural strength (VSN 77 103 or ISO R 178); DB = bending at rupture; SB = impact bending strength (VSN 77 105).

(a) catalyst: 1-methylimidazole (No. 11 with 2 wt.%, Nos. 12-16 with 4 wt.2); (b) accelerator: tetramethylammonium chloride.

LT 2067

Table 4

Effect of the cross-linked structure on the torsional adhesive strength TAS, and the parameters A, B, C of the cohesive strength (equation (7)).

Epoxy resin (basic structure)	Hardener	T <sub>g</sub> °C	A K	C N mm <sup>-2</sup> K <sup>-1</sup>	B N mm <sup>-2</sup>	TAS (77 K) N mm <sup>-2</sup> calc.   exp.
1 	Catalyst: Zn-amine complex	160	44	0.55	265	222   227
2 As for 1		159	31	0.54	250	208   214
3 50 wt.-% BADG (a) +50 wt.-% DGH (b)		160	35	0.57	266	222   208
4 As for 1		130	38	0.59	262	215   208
5 As for 1 + 15 wt.-% polyester		119	38	0.53	229	190   181
6 		90	65	0.58	248	204   202
7 AW 136 (d)	HY 994 (d)	77	45	0.64	254	204   193
8 AV 138 (without filler) (d)	HV 998 (d)	90	80	0.56	247	203   192

(a) BADG = bisphenol A diglycidylether. (b) DGH = 1,3-diglycidyl-5,5-dimethylhydantoin.

(c) Linear polymer of Union Carbide; trade name: 'Phenoxyl'.

(d) AW 136/HY 994 and AV 138/HV 998 are technical, formulated systems based on BADG and aliphatic amines for special application in the adhesives area.

Table 5  
EVALUATION OF YIELD STRESS MEASUREMENTS ON POLYCARBONATES

No.	$\dot{\epsilon}/s^{-1}$	A/K	$B/(N\ mm^{-2})$	$C/(N\ mm^{-2}\ K^{-1})$	$(A + T_g)/K$
1	$10^{-5}$	43	157.5	0.3417	461
2	$10^{-3}$	73	157.7	0.3211	491
3	$10^{-1}$	105	157.9	0.3000	523

LT 2067

Table 6  
EFFECT OF THE CROSS-LINKED STRUCTURE ON THE  $T_g$  AND THE CONSTANTS A, B AND C FROM EQUATION (7)

No.	Type of hardener	Cured by	Epoxy resin (basic structure)	$T_g$ (TMA) °C	A K	B $\text{K mm}^{-2}$	C $\text{K mm}^{-2} \text{K}^{-1}$
1	Aromatic amine			159	31	250	0.54
2				177	43	284	0.58
3				35	26	293	0.88
4			as for 1	148	17	270	0.62
5			as for 2	170	42	279	0.57
6			as for 1	205	27	258	0.52
7			as for 2	219	46	277	0.50
8	Aliphatic amine	Triethylenetetramine	as for 1	125	45	271	0.51
9		trimethylhexamethylenediamine	as for 1	100	46	195	0.7
10	Anhydride		as for 1	130	18	262	0.59
11				227	11	182	0.36
12	Catalytic	1-methylimidazole	as for 1	142	44	241	0.53
13				166	48	253	0.52
14	Phenol		as for 13	158	44	252	0.53
15				90	65	248	0.58
16	Dicyclic amide		as for 1	120	87	251	0.52
17			as for 1 (JD 981)	94	69	255	0.58
	Mean value			145	43	253	0.56

(a) linear polymer of Union Carbide, trade name: 'Phenoxyl'; (b) formulated version of system 16, commercial product of CIBA-GEIGY AG.

Table 7

Effect of plasticisers on the glass transition temperature  $T_g$  measured by thermomechanical analysis (TMA) and torsional pendulum tests ( $\Lambda_{max}$ ), on the mechanical strength and on the parameters B and C of the cohesive strength in epoxy resins based on bisphenol-A-diglycidyl-ether and hexahydrophthalic anhydride.

Plasticiser	$T_g$ (TAS) $^{\circ}\text{C}$	$T_g$ ( $\Lambda_{max}$ ) $^{\circ}\text{C}$	FS ( $23^{\circ}\text{C}$ ) $\text{N mm}^{-2}$ (a)	TAS ( $23^{\circ}\text{C}$ ) $\text{N mm}^{-2}$ (b)	C $\text{N mm}^{-2} \text{K}^{-1}$	B $\text{N mm}^{-2}$	$K_{IC}$ ( $23^{\circ}\text{C}$ ) $\text{MN m}^{-3/2}$ (c)
-	120-140	143	136	83	0.59	262	0.56
15 wt.% adipic acid polyester	104-133	128	123	72	0.53	220	0.74
15 wt.% oligoester of dimeric aliphatic acid	102-134	132	115	66	0.51	218	0.85
15 wt.% butadiene-acrylonitrile copolymer	108-137	134	114	63	0.45	194	1.16
15 wt.% ABS powder	118-140	142	98	71	0.46	206	1.30

(a) FS = flexural strength

(b) TAS = torsional adhesive strength

(c)  $K_{IC}$  = critical stress intensity factor



## REFERENCES

<u>No.</u>	<u>Author</u>	<u>Title, etc</u>
1	H. Batzer F. Lohse R. Schmid	<i>Angew. Makromol. Chem.</i> , <u>29/30</u> , 349 (1973)
2	F. Lohse R. Schmid	<i>Chimia</i> , <u>28</u> , 576 (1974)
3	H. Batzer F. Lohse R. Schmid	<i>Angew. Makromol. Chem.</i> , <u>29/30</u> , 349, p 354 (1973)
4	H. Batzer F. Lohse	Ullmanns Enzyklopadie der technischen Chemie. 4. Auflage, Verlag Chemie GmbH, Weinheim 1975, <u>10</u> , p 563f
5	Y. Tanaka T.F. Mika	C.A. May, Y. Tanaka (Ed): Epoxy Resins, Chemistry and Technology. Marcel Dekker Inc., New York, p 135f, 239f (1973)
6	W. Fisch W. Hofmann	<i>J. Polym. Sci.</i> , <u>12</u> , 497 (1954)
7	W. Fisch W. Hofmann	<i>Makromol. Chem.</i> , <u>44-46</u> , 8 (1961)
8	E.C. Dearborn R.M. Fuoss A.F. White	<i>J. Polym. Sci.</i> , <u>16</u> , 201 (1955)
9	Y. Tanaka H. Kakiuchi	<i>J. Appl. Polym. Sci.</i> , <u>7</u> , 1063 (1963)
10	L. Shechter J. Wynstra R.P. Kurkijy	<i>Ind. Eng. Chem.</i> , <u>48</u> , 94 (1956)
11	K. Dusek M. Bleha S. Lunak	<i>J. Polym. Sci., Polym. Chem. Ed.</i> , <u>15</u> , 2393 (1977)
11a	J.T. Smith	<i>Polymer</i> , <u>2</u> , 95 (1961)
12	J. Eichler J. Mleziva	<i>Angew. Makromol. Chem.</i> , <u>19</u> , 31 (1971)
13	L. Shechter J. Wynstra	<i>Ind. Eng. Chem.</i> , <u>48</u> , 86 (1956)
14	T.F. Mika	C.A. May, Y. Tanaka (Ed): Epoxy Resins, Chemistry and Technology. Marcel Dekker Inc., New York, p 268 (1973)

## REFERENCES (continued)

<u>No.</u>	<u>Author</u>	<u>Title, etc</u>
15	H. Fink	<i>Plaste Kautsch.</i> , <u>17</u> , 677 (1970)
16	H. Batzer W. Fisch	<i>Kautsch. Gummi. Kunstst.</i> , <u>17</u> , 563 (1964)
17	A.J. Sein J. Rietberg J.M. Schouten	Unilever NV, Erf. German Patent 2.163.962 <i>Chem. Abstr.</i> , <u>77</u> , p 103473a (1972)
18	A.M. Eastham	<i>Fortschr. Hochpolym-Forsch.</i> <u>2</u> , 18 (1960)
19	P. Nowak M. Saure	<i>Kunststoffe</i> , <u>54</u> , 557 (1964)
20	J.J. Harris S.C. Temin	<i>J. Appl. Polym. Sci.</i> , <u>10</u> , 523 (1966)
21	W. Hofmann	Unpublished results
22	T.F. Saunders M.F. Levy J.F. Serino	<i>J. Polym. Sci.</i> , Part A-1, <u>5</u> , 1609 (1967)
23	P. Eyerer	<i>J. Appl. Polym. Sci.</i> , <u>15</u> , 3067 (1971)
24	S.A. Zahir	Unpublished results
25	J.H. Flynn L.A. Wall	<i>J. Polym. Sci.</i> , Part B, <u>4</u> 323 (1966)
26	W. Fisch W. Hofmann R. Schmid	<i>J. Appl. Polym. Sci.</i> , <u>13</u> 295 (1969)
27	R. Schmid	<i>Prog. Colloid Polym. Sci.</i> , <u>64</u> , 17 (1978)
28	R. Schmid	Mitteilungen des chem. Forschungsinstitutes der Wirtschaft Österreichs u.d. österreichischen Kunststoffinstitutes'. (Austrian Chem. Research Institute and Plastics Institute), 4. Danube Regions Discussion, p 43, October 1971.
29	L.E. Nielsen	<i>J. Macromol. Sci. Rev. Macromol. Chem.</i> , <u>3</u> , 69 (1969)
30	D.W. van Krevelen	Properties of Polymers. 2 Edition, Elsevier Sci. Publ. Comp., Amsterdam, Oxford, New York (1976)
31	H. Batzer U. Kreibich	Publication in preparation.
32	G.A. Pogany	<i>Polymer</i> , <u>11</u> , 66 (1970)
33	Y.M. Blyakhman T.J. Borisova T.M. Levitskaya	<i>Vysokomol. Soedin.</i> , Ser.A: <u>12</u> , 1544 (1970)

## REFERENCES (continued)

<u>No.</u>	<u>Author</u>	<u>Title, etc</u>
34	R. Schmid F. Lohse W. Fisch H. Batzer	<i>J. Polym. Sci., Part C</i> , <u>30</u> , 339 (1970)
35	J. Kaiser	<i>Makromol. Chem.</i> , <u>180</u> , 573 (1979)
36	M. Fischer R. Schmid	K.W. Allen (Ed), <i>Adhesion 3</i> , Applied Science Publishers Ltd, London, pp 31-52 (1979)
37	A. Puck	Publication in preparation
38	P.B. Bowden	R.N. Haward (Ed), <i>The Physics of Glassy Polymers</i> , Applied Science Publishers Ltd, London, pp 279-339 (1973)
39	D.H. Kaelble	<i>Physical Chemistry of Adhesion</i> . Wiley-Interscience, New York, London, Sydney, Toronto, pp 349-395 (1971)
40	R.A. Duckett S. Rabinowitz J.M. Ward	<i>J. Mater. Sci.</i> , <u>5</u> , 909 (1970)
41	S.S. Sternstein L. Ongchin A. Silverman	<i>Appl. Polym. Symp.</i> , <u>7</u> , 175 (1968)
42	I. Szabó	<i>Einführung in die Technische Mechanik</i> . (Introduction to technical mechanics). Springer Verlag, Berlin, Heidelberg, New York, p 95ff (1975)
43	D. Evans J.T. Morgan G.B. Stapleton	<i>Epoxy resins for superconducting magnet encapsulation</i> . Rutherford Laboratory Report SBN 902376454 (1972)
44	C. Bauwens-Crowet J.C. Bauwens G. Homes	<i>J. Polym. Sci., Part A-2</i> , <u>7</u> , 735 (1969)
45	J.A. Roetling	<i>Polymer</i> , <u>6</u> , 311 (1965)
46	C. Bauwens-Crowet J.C. Bauwens G. Homes	<i>J. Mater. Sci.</i> , <u>7</u> , 176 (1972)
47	R.E. Robertson	<i>Appl. Polym. Symp.</i> , <u>7</u> , 201 (1968)
48	A.S. Argon	<i>Philos. Mag.</i> , <u>28</u> , 839 (1973)
49	A.S. Argon	P.H. Geil, E. Baer, Y. Wada (Ed). <i>The solid state of polymers</i> . Marcel Dekker, Inc., New York, pp 573-596 (1974)

## REFERENCES (concluded)

- | <u>No.</u> | <u>Author</u>  | <u>Title, etc</u>  |
|------------|--|--|
| 50         | A.S. Argon<br>N.I. Bessonov                              | <i>Polym. Eng. Sci.</i> , <u>17</u> , 174 (1977)   |
| 51         | J.C. Bauwens   | <i>J. Polym. Sci.</i> , Part A-2, <u>5</u> , 1145 (1967)   |
| 52         | T.E. Brady<br>G.S.Y. Yeh                                 | <i>J. Appl. Phys.</i> , <u>42</u> , 4622 (1971)  |
| 53         | J.O. Hirschfelder<br>C.F. Curtiss<br>R.B. Bird           | Molecular Theory of Gases and Liquids.<br>John Wiley & Sons, Inc., New York, London, Sydney, pp 624-630<br>(1964)                                    |
| 54         | I.M. Ward  | <i>J. Polym. Sci.</i> , Polym. Symp, <u>32</u> , 195 (1971)  |
| 55         | S. Turner  | R.N. Haward (Ed), The Physics of the Glassy State.<br>Applied Science Publishers Ltd, p 232 (1973)   |
| 56         | I.M. Ward  | <i>J. Mater. Sci.</i> , <u>6</u> , 1397 (1971)   |
| 57         | M. Gordon  | P.D. Ritchie (Ed), 'Physics of Plastics'.<br>The Plastics Institute, London, p 226ff (1965)  |
| 58         | M.R. Carpenter<br>D.B. Davies<br>A.J. Matheson           | <i>J. Chem. Phys.</i> , <u>46</u> , 2451 (1967)  |
| 59         | H.A. Stuart  | Die Struktur des freien Molekuls. (The structure of free<br>molecules).<br>Springer-Verlag, Berlin, Göttingen, Heidelberg, p 65ff (1952)             |
| 60         | D.W. van Krevelen  | Properties of polymers. 2nd Edition<br>Elsevier Sci., Publ. Comp., Amsterdam, Oxford, New York,<br>p 136 (1976)                                      |
| 61         | A. Tobolsky<br>H. Hoffman                                | Mechanische Eigenschaften und Struktur von Polymeren.<br>(Mechanical properties and structure of polymers)<br>Berliner Union, Stuttgart, p 88 (1967) |
| 62         | A. Bondi   | Physical Properties of Molecular Crystals, Liquids and Gases.<br>John Wiley & Sons, Inc., New York, London, Sydney, p 27,<br>(1973)                  |
| 63         | H. Spähn<br>H.W. Lenz                                    | <i>Z. Werkstofftech.</i> , <u>4</u> , 16 (1973)  |
| 64         | F. Kerkhof   | <i>Kolloid-Z. Polym.</i> , <u>251</u> , 545 (1973)   |
| 65         | A.C. Meeks   | <i>Br. Polym. J.</i> , <u>7</u> , 1 (1975)   |
| 66         | W.D. Bascom<br>R.J. Moulton<br>E.H. Rowe<br>A.R. Siebert | <i>Am. Chem. Soc., Div. Org. Coat. Plast. Chem. Pap.</i> , <u>39</u> , 164<br>(1978)   |

REPORTS CITED ARE NOT NECESSARILY  
AVAILABLE TO MEMBERS OF THE PUBLIC  
OR TO COMMERCIAL ORGANISATIONS

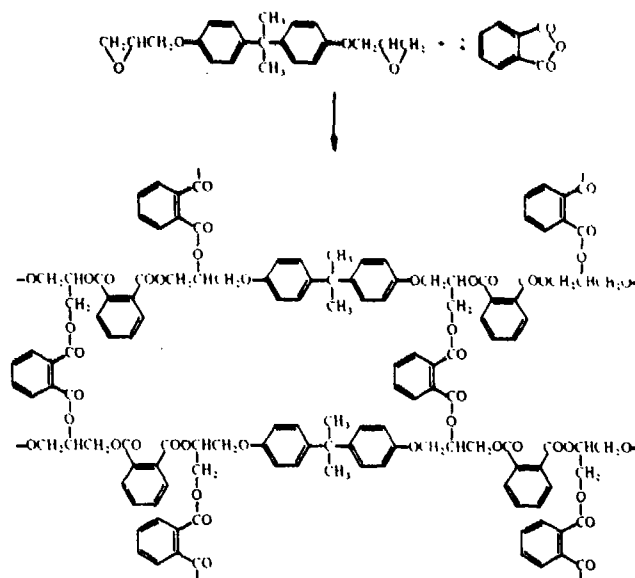


Fig 1 Cross-linking scheme for bisphenol A diglycidyl ether cross-linked with phthalic anhydride

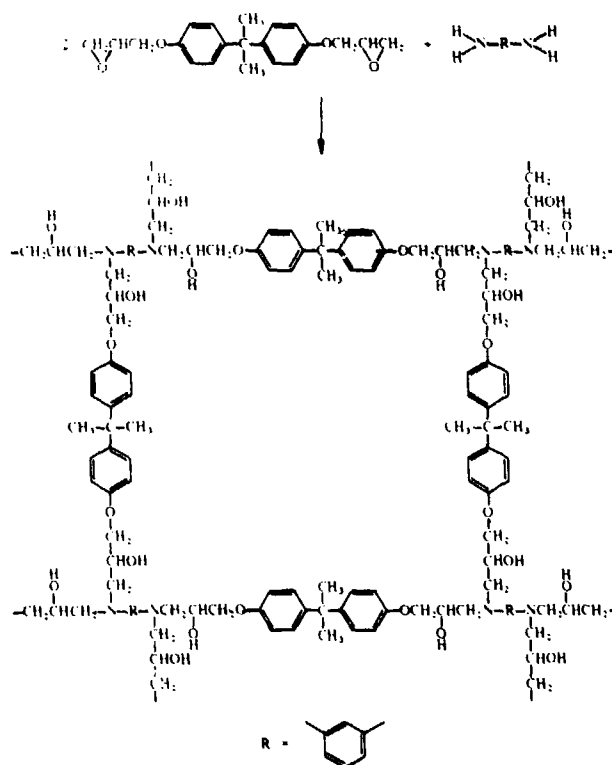


Fig 2 Cross-linking scheme for bisphenol A diglycidyl ether cross-linked with a primary aromatic diamine

Figs 3&4

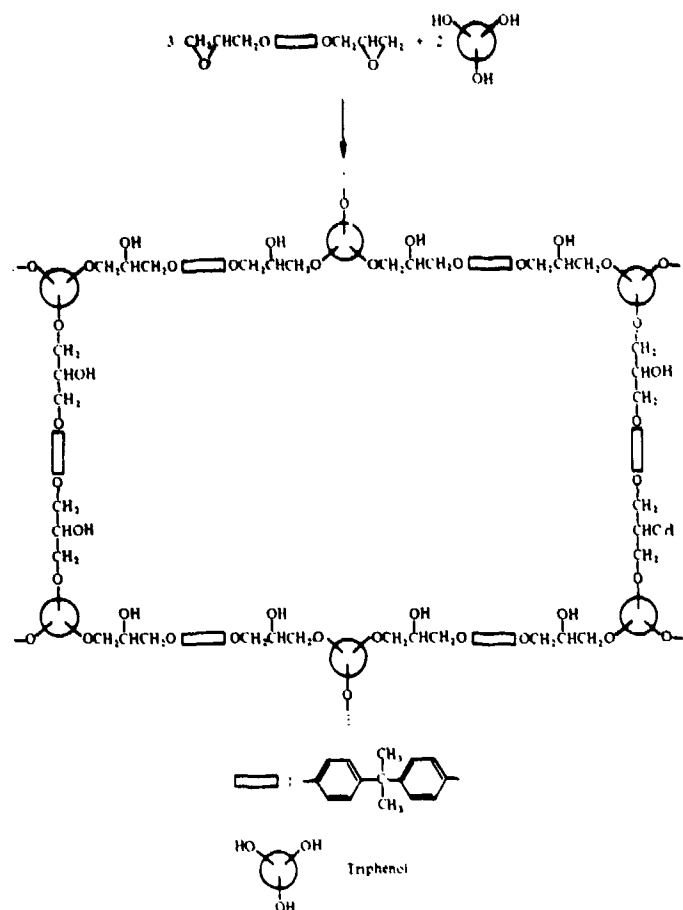


Fig 3 Schematic illustration of the structure obtained upon cross-linking bisphenol A diglycidyl ether with a triphenol (pyrogallol, phloroglucine, etc)

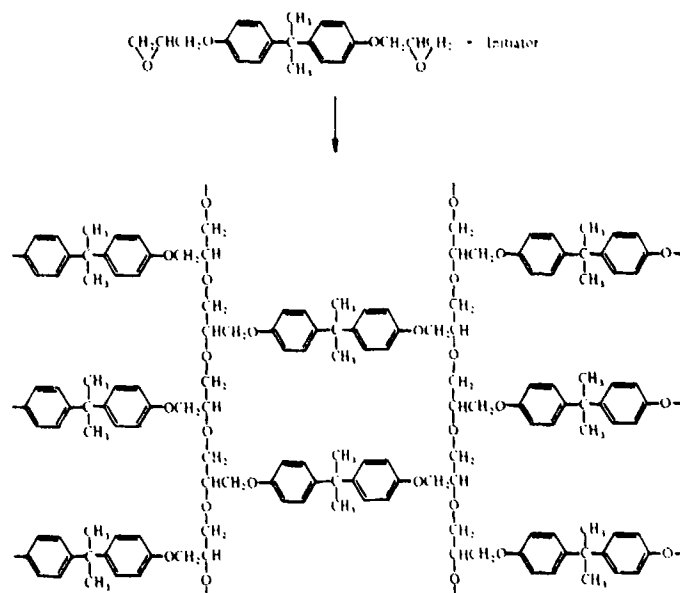


Fig 4 Cross-linking scheme for a product obtained by polymerisation of epoxy groups

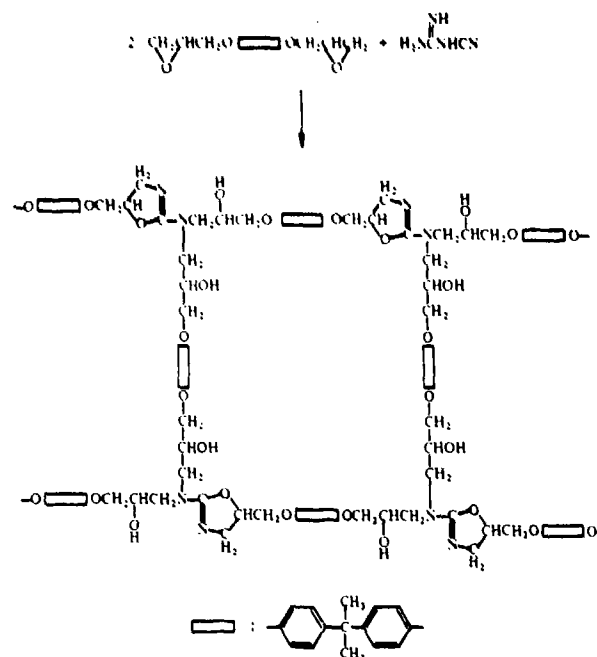


Fig 5 Cross-linking scheme for a product obtained by cross-linking bisphenol A diglycidyl ether with dicyandiamide. Representation of the structural component produced with formation of oxazoline derivatives

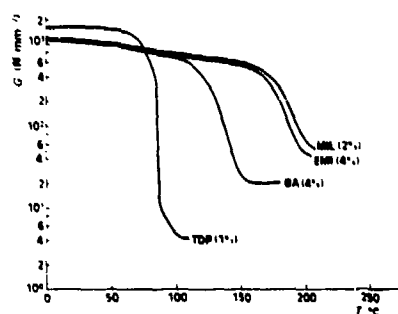


Fig 6 Curve of the modulus of shear  $G$  against temperature, for bisphenol A diglycidyl ether cross-linked with different polymerisation initiators (MIL = 1-methylimidazole; EMI = 2-ethyl-4-methylimidazole; BA = borontrifluoride-amine complex; TDP = tris(2,4,6-dimethylaminomethyl)phenol. Percentage data are in wt %.

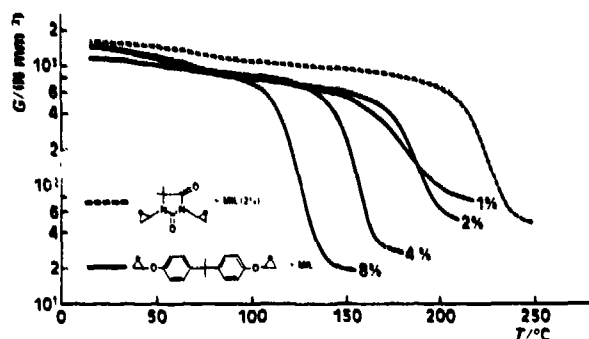


Fig 7 Effect of the concentration of 1-methylimidazole (MIL) on the modulus of shear curves of epoxy resins obtained from bisphenol A diglycidyl ether and 1,3-diglycidyl-5,5-dimethylhydantoin. Percentage data are in wt %.

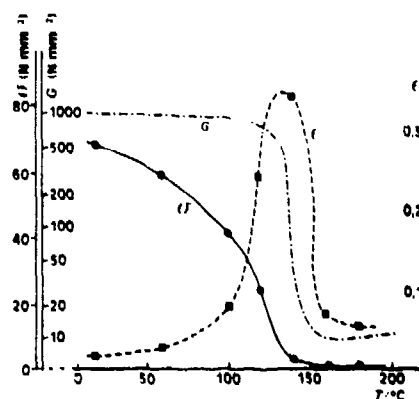


Fig 8 Temperature dependence of the modulus of shear  $G$ , the tensile strength  $\sigma$  and the elongation at break  $\epsilon$  of the epoxy resin obtained from bisphenol A diglycidyl ether and hexahydrophthalic anhydride

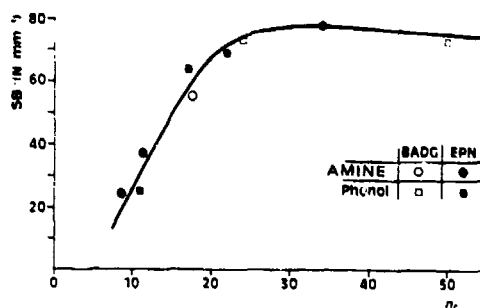


Fig 9 Dependence of the impact strength  $SB$  of epoxy resins on the mean number of atomic distances between the cross-linking positions  $n_c$ . BADG: bisphenol A diglycidyl ether,  $n = 0.15$  and  $2$  (see Table 3), EPN: epoxy novolak, Amine: primary aromatic diamine, Phenol: di- and tri-phenol



Fig 10 Apparatus for testing the torsional adhesive strength (TAS)





- Fig 11 Temperature dependence of the torsional adhesive strength (TAS)<sup>†</sup>, the flexural strength (FS)<sup>†</sup> and the tensile strength (TS)<sup>†</sup> of an epoxy resin obtained from bisphenol A diglycidyl ether (BADG), cured with hexahydrophthalic acid and accelerator, 1 wt % of benzyldimethylamine

† English abbreviations  
\* German abbreviations

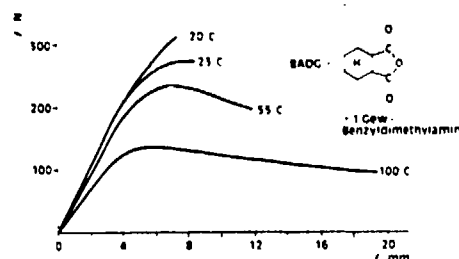
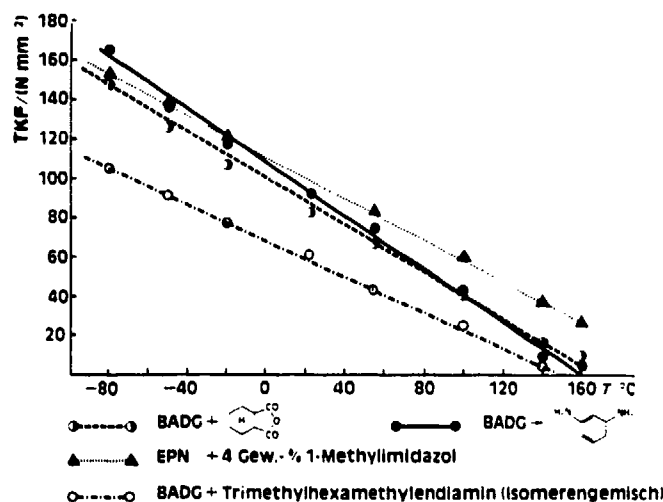


Fig 12 Temperature dependence of the stress-strain curve for an epoxy resin obtained from bisphenol A diglycidyl ether (BADG) cured with hexahydrophthalic anhydride and accelerator, 1 wt % benzylidimethylamine (F = force; f = bending)

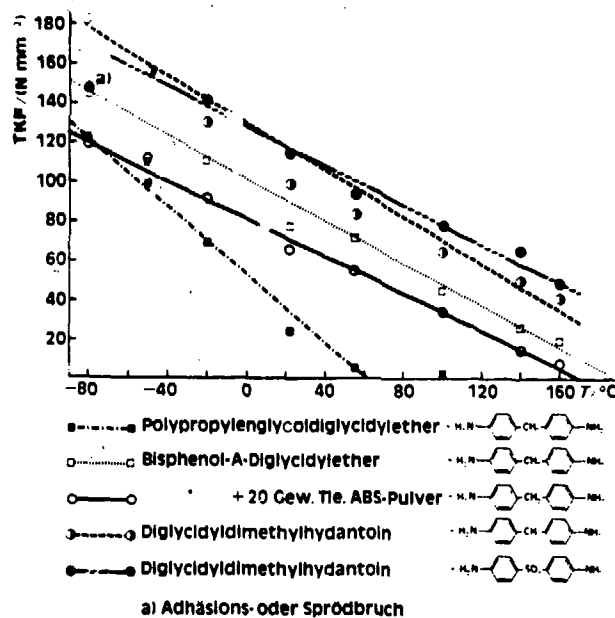


Key:

- ▲.....▲ EPN + 4 wt % methylimidazole
- .....○ BADG + trimethylhexamethylenediamine (isomeric mixture)

Fig 13 Torsional adhesive strength (TKF)\* versus temperature (T)-curve of epoxy resins obtained from bisphenol A diglycidyl ether (BADG) and epoxy novolaks (EPN) for different types of hardener (MIL = 1-methylimidazole; TMD = trimethylhexamethylenediamine (isomeric mixture))

\* German abbreviation



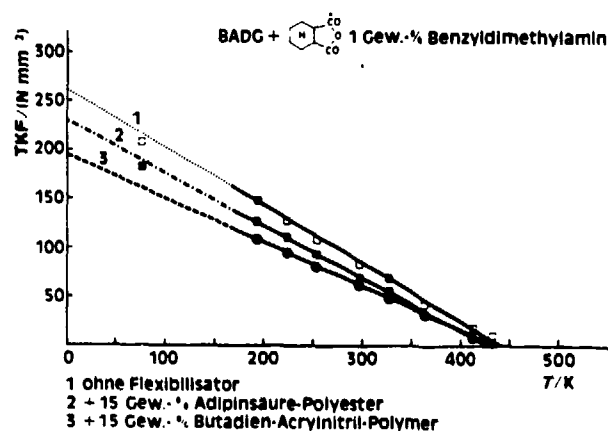
## Key:

- - - - ■ polypropyleneglycoldiglycidyl ether + ...
- - - - □ bisphenol A diglycidyl ether + ...
- - - - ○ bisphenol A diglycidyl ether + 20 parts by weight of ABS-powder + ...
- - - - ● diglycidylidimethylhydantoin + ...
- - - - ● diglycidylidimethylhydantoin + ...

(a) adhesive or brittle fracture

Fig 14 Effect of the structure of epoxy resins on the torsional adhesive strength (TKF)\* versus temperature (T)-curve

\* German abbreviation



## Key:

- 1 Without plasticiser
- 2 + 15 wt % adipic acid polyester
- 3 + 15 wt % butadiene-acrylonitrile polymer

BADG + ... 1 wt % benzylidimethylamine

Fig 15 Effect of plasticiser on the torsional adhesive strength (TKF)\* versus temperature (T)-curve

\* German abbreviation

ADVANCE DISTRUBUTION:

RMCS  
ITC  
DRIC 70

BAe, Hatfield  
Library, NGTE

RAE

Deputy Director  
Main Library  
Materials Dept 12